CIMAC CONGRESS 25
ZURICH, MAY 19 – 23, 2025

2025 | 524

A COMPUTATIONAL STUDY OF METHANOL COMBUSTION CHEMISTRY AT HIGH PRESSURES

Simulation Technologies, Digital Twins and Complex System Simulation

Lambros Kaiktsis, University of Doha for Science and Technology

Theodora Syrrou, National Technical University of Athens
Dimitris Kazangas, National Technical University of Athens
Dionysios Kolaitis, National Technical University of Athens
Maria Founti, National Technical University of Athens

DOI: https://doi.org/10.5281/zenodo.15209596

ABSTRACT

The present study investigates methanol (CH3OH) combustion under CO2 supercritical conditions (s-CO2), a topic of current interest for gas turbine applications in the context of greenhouse gas (GHG) emissions reduction and relevant for marine applications. The study is computational and assesses a reduced-order chemical kinetic mechanism for methanol combustion applications across a wide range of pressure, temperature, and fuel-air equivalence ratios, typical of dual-fuel marine engines and gas turbines.

The reduced-order mechanism ACR55 of Pichler & Nilsson (2018) was evaluated through comparison with experimental data, as well as against the computational results of the detailed mechanism Updated HP-Mech of Wang et al. (2022). The following problems have been considered: (a) premixed laminar flame, (b) ignition of homogeneous mixtures, and (c) combustion at Perfectly Stirred Reactor (PSR) conditions. Standard mixtures considered in the experiments (methanol in air/O2 and O2/Ar as diluent) were used.

The computational results obtained from the two mechanisms were evaluated by comparison with experimental data in the context of the above three standard problems. The computational results have proven a very good performance of the reduced ACR55 mechanism, which is demonstrated by the good comparison against the experimental data and the detailed mechanism Updated HP-Mech, for all three problems investigated.

The effect of CO2 as diluent was studied for the PSR and laminar flame problems, by considering: (a) N2 as diluent, and (b) s-CO2 as diluent, at the same conditions, which include representative gas turbine and marine dual-fuel engine operation. In particular, the following range was considered: pressures of 175 – 250 atm, initial temperatures (mainly) of 1,300 – 1,800 K, equivalence ratios of 0.5 – 2.0. The main findings of the present computations can be summarized as follows.

(i) Combustion at PSR conditions: the two mechanisms produce comparable results in the entire range of conditions investigated. For all mixtures, the produced CO2 is higher for N2 as diluent. For rich mixtures, a partial decomposition of the added CO2 is observed.

(ii) Premixed laminar flames: for unburned mixture temperatures of 600 K and 700 K, the laminar flame speed is significantly higher for N2 dilution, for all stoichiometries considered. For unburned mixture temperature of 1,800 K and lean mixtures, the laminar flame speed remains higher for N2 dilution, however the differences are less pronounced; for rich mixtures, the laminar flame speed is substantially higher for N2 dilution.

For the two problems studied, representative cases were characterized by performing rate of production (ROP) analysis, for identifying the principal chemical pathways. Here, the following cases were analyzed: (i) Combustion at PSR conditions: T=1500 K, p=220 bar, ?=0.8 and ?=2.0. (ii) Premixed laminar flame: unburned mixtures with T=700 K and T=1,800 K, ?=0.5, p=200 atm and p=220 atm. The results of ROP analysis identify the chemical paths of important species and explain the observed differences regarding the effects of N2- and s-CO2 dilution.

Paper No. 524

A Computational Study of Methanol Combustion Chemistry at High Pressures

Lambros Kaiktsis, University of Doha for Science and Technology, National Technical University of Athens, Greece
Theodora Syrrou, National Technical University of Athens, Greece
Dimitris Kazangas, National Technical University of Athens, Greece
Dionysios Kolaitis, National Technical University of Athens, Greece
Maria Founti, National Technical University of Athens, Greece

ABSTRACT

The present study investigates methanol (CH_3OH) combustion under CO_2 supercritical conditions (s-CO_2), a topic of current interest for gas turbine applications in the context of greenhouse gas (GHG) emissions reduction and relevant for marine applications. The study is computational and assesses a reduced-order chemical kinetic mechanism for methanol combustion applications across a wide range of pressure, temperature, and fuel-air equivalence ratios, typical of dual-fuel marine engines and gas turbines.

The reduced-order mechanism *ACR55* by Pichler & Nilsson (2018) was evaluated through comparison with experimental data, as well as against the computational results of the detailed mechanism *Updated HP-Mech* of Wang et al. (2022). The following problems have been considered: (a) premixed laminar flame, (b) ignition of homogeneous mixtures, and (c) combustion at Perfectly Stirred Reactor (PSR) conditions. Standard mixtures considered in the experiments (methanol in air/O_2 and O_2/Ar as diluent) were used.

The computational results obtained from the two mechanisms were evaluated by comparison with experimental data in the context of the above three standard problems. The computational results have proven a very good performance of the reduced *ACR55* mechanism, which is demonstrated by the good comparison against the experimental data and the detailed mechanism *Updated HP-Mech*, for all three problems investigated.

The effect of CO_2 as diluent was studied for the PSR and laminar flame problems, by considering: (a) N_2 as diluent, and (b) s-CO_2 as diluent, at the same conditions, which include representative gas turbine and marine dual-fuel engine operation. In particular, the following range was considered: pressures of 175 – 250 atm, initial temperatures (mainly) of 1300 – 1800 K, equivalence ratios of 0.4 – 2.0. The main findings of the present computations can be summarized as follows.

i. Combustion at PSR conditions: The two mechanisms produce comparable results in the entire range of conditions investigated. For all mixtures, the produced CO_2 is higher for N_2 as diluent. For rich mixtures, a partial decomposition of the added CO_2 is observed.

ii. Premixed laminar flames: For unburned mixture temperatures of 600 K and 700 K, the laminar flame speed is significantly higher for N_2 dilution, for all stoichiometries considered. For unburned mixture temperature of 1800 K and lean mixtures, the laminar flame speed remains higher for N_2 dilution, however the differences are less pronounced; for rich mixtures, the laminar flame speed is substantially higher for N_2 dilution.

For the two problems studied, representative cases were characterized by performing Rate Of Production (ROP) analysis, for identifying the principal chemical pathways. Here, the following cases were analyzed: (i) Combustion at PSR conditions: T=1500 K, P=220 bar, φ=0.5. (ii) Premixed laminar flame: unburned mixture with T_{un}=700 K, φ=0.5, P=220 atm. The results of ROP analysis identify the chemical paths of important species and explain the observed differences regarding the effects of N_2 and s-CO_2 dilution.

INTRODUCTION

The International Maritime Organization (IMO) has outlined a comprehensive roadmap in its 2023 GHG Strategy, targeting net-zero greenhouse gas (GHG) emissions by 2050 (MEPC.377(80) [1]). The strategy includes intermediate targets of reducing CO_2 emissions by 40% until 2030, relative to 2008 levels. IMO intends to also incorporate methane (CH_4) and nitrous oxide (N_2O) in future quantification of GHG emissions from shipping. For quantifying ship performance in the context of GHG emissions, IMO has introduced proper performance indices, namely the Energy Efficiency Design Index (EEDI), the Energy Efficiency Existing Ship Index (EEXI), and the Carbon Intensity Indicator (CII) [1]. EEDI, in effect from January 1, 2013, evaluates and regulates energy efficiency of newbuildings; it specifies the energy efficiency range of new ships based on their size and type, considering average efficiency data from vessels built between 1999 and 2009.

To address emissions from existing ships, IMO introduced EEXI as an amendment to MARPOL Annex VI, effective January 1, 2023. EEXI commonly expresses CO_2 emissions per tonne of vessel Deadweight over one nautical mile, which should not exceed a required threshold. Finally, CII, also mandatory as of January 1, 2023, evaluates operational carbon intensity based on GHG emissions per tonne of vessel Deadweight over one nautical mile. The outcome of the CII calculation corresponds to a rating level (A, B, C, D, or E), which becomes progressively stricter over time, potentially requiring improvement (retrofit) actions. Together, these measures represent critical steps in the IMO's strategy to reduce the environmental impact of shipping.

In addition to CO_2, the IMO has focused on reducing nitrogen oxides (NO_x) and sulfur oxides (SO_x) emissions from marine operations. To address these pollutants, the IMO established Nitrogen Oxide Emission Control Areas (NECAs) and Sulfur Oxide Emission Control Areas (SECAs), where stricter regulations are enforced. As of January 1, 2015, four SECAs have been designated: the Baltic Sea, North Sea, North America, and the Caribbean Sea (MEPC.176(58) [2]). Regulation 14 of Annex VI of the 1997 MARPOL Protocol specifies sulfur emission factors and imposes limits on sulfur content in fuel, both globally and within SECAs [2]. Since January 2020, the global sulfur content limit in fuel has been reduced from 3.5% to 0.5% by mass. Within SECAs, stricter requirements have reduced the limit to 0.1% by mass (MEPC.320 (74) [3]).

For NO_x emissions, IMO implemented the Tier (I, II and III) standards, which regulate NO_x emissions based on the ship's construction date and engine speed [2, 4]. Tier III standards apply to engines on ships built after January 1, 2016, operating in NECAs, with a NO_x limit of 3.4 g/kWh for low-speed engines (n < 130 rpm), which is approximately 80% lower than Tier I standards.

Methanol (CH_3OH) has emerged as a viable solution for meeting the strict emission regulations in the maritime and energy sectors. One current implementation of methanol is its use as a fuel in gas turbines, where it offers significant environmental benefits [5-6]. A key aspect of methanol's sustainability lies in the implementation of a production process that utilizes renewable energy and CO_2 recycling to generate a cleaner fuel alternative. The production of green methanol begins with renewable electricity from sources like wind turbines [7] and solar panels, which are used for water electrolysis. Part of the exhaust gases from gas turbines is captured and utilized for methanol synthesis through the reaction of CO_2 with H_2. The remaining CO_2, along with O_2 and methanol, is introduced into the gas turbine combustion chamber under supercritical CO_2 conditions [8-9]. This can lower the combustion temperature, resulting in reduced NO_x and CO_2 emissions. Additionally, the overall CO_2 emissions are nearly eliminated, making methanol a sustainable and environmentally friendly option for the energy transition. Similarly, methanol could be used as a green alternative for marine engines [10-11]. In this case, a carbon capture process would need to be implemented for the CO_2 produced by combustion, a process which requires cooling the CO_2 before capture, typically to 40-60°C.

In the above context, the present work aims to verify the new combustion concepts and characterize combustion through extensive chemical kinetics calculations. Chemical kinetic mechanisms are commonly validated against experimental data to ensure that they can reproduce the key features of combustion. In this context, two chemical kinetic mechanisms have been used to simulate the combustion of methanol. In particular, the reduced-order mechanism *ACR55* by Pichler & Nilsson (2018) [12] is used as the main research tool, after a comprehensive evaluation against the results obtained using the detailed mechanism *Updated HP-Mech* by Wang et al. (2022) [13], as well as against literature experimental data.

The following problems have been considered: (a) premixed laminar flame, (b) ignition of homogeneous mixtures, and (c) combustion under Perfectly Stirred Reactor (PSR) conditions. The results demonstrate the very good performance of the reduced *ACR55* mechanism, as evidenced by its very good agreement with both experimental data and the detailed *Updated HP-Mech* mechanism for the problems investigated. Due to its good performance, the *ACR55* mechanism is subsequently used to study methanol combustion under supercritical conditions. The present study is completed by analyzing representative cases by means of Rate of Production (ROP) analysis, yielding the principal chemical pathways of methanol combustion at supercritical CO_2 conditions.

METHODOLOGY OUTLINE

The *ACR55* reduced-order mechanism of Pichler & Nilsson (2018) [12], which has been shown to perform well for internal combustion engine applications, is used as the main tool in the present study. The mechanism is validated against: (i) the *Updated HP-Mech* detailed mechanism by Wang et al. (2022) [13], which builds on a previous version adapted for high pressures, and (ii) literature experimental data. Three reference problems have been considered:

(a) Premixed laminar flame, using the experimental data of Zhang et al. (2008) [14] and Beeckman et al. (2014) [15] for validation. The data refer to pressures in the range P=1–10 bar, unburned mixture temperatures T_{un}=298–423 K, and equivalence ratios φ=0.7–1.5.

(b) Ignition of homogeneous mixtures, using the shock tube experimental results of Burke et al. (2016) [16], for conditions P=1.96-51 atm, T=950-1475 K, and φ=0.5, 1.0, 2.0.

(c) Combustion under Perfectly Stirred Reactor (PSR) conditions. Here, species temperature profiles of Jet Stirred Reactors (JSRs) were used from the experiments of Wang et al. (2022) (P=10 atm, 100 atm, T = 550–950 K, and φ = 0.1, 1.0, 9.0) and Burke et al. (2016) (P=10 atm, 20 atm, T=550–950 K, and φ = 0.2, 0.5, 1.0, 2.0).

For all three problems, the present simulations employed the mixtures of the experiments (methanol in air/O_2 and O_2/Ar as a diluent). The present computational results have demonstrated that the *ACR55* reduced mechanism results, in all cases, in low levels of the relative error, with reference to both the experiments and the detailed *Updated HP-Mech* mechanism. Thus, the *ACR55* mechanism was subsequently used to study methanol combustion under supercritical conditions.

The focus of the present study concerns the effect of CO_2 as a diluent under supercritical conditions. Two reference problems are considered: (a) premixed laminar flame, and (b) combustion under Perfectly Stirred Reactor (PSR) conditions. For both problems, dilution is attained in terms of: (i) N_2, and (ii) supercritical CO_2 (s-CO_2); the same conditions are considered for the two dilutants. These conditions include representative gas turbine and marine dual-fuel engine operating conditions, specifically, pressures of 175–250 atm, initial temperatures in the range 1300–1800 K, and equivalence ratios of 0.4–2.0. It is noted that, to our knowledge, no experimental data for methanol ignition and combustion under supercritical conditions with the addition of CO_2 as a diluent have been reported in the open literature.

For the two prototype problems studied, representative cases are analyzed using Rate of Production (ROP) analysis, to identify the principal chemical pathways. In particular, the following cases are considered: (i) combustion under PSR conditions at T=1500 K, P=220 bar, with equivalence ratio φ=0.5; (ii) premixed laminar flame, with unburned mixture temperature T_{un}=700 K, with φ=0.5, at pressure of P=220 atm. The ROP analysis of the present study identifies the chemical pathways of key species and explains the observed differences between N_2 and s-CO_2 dilution effects.

MECHANISM ASSESSMENT

The large set of validation experimental data of CH_3OH combustion outlined in the previous Section encompass ignition delay times (IDT), concentration profiles in Jet Stirred Reactors (JSRs), and values of laminar flame speed (LFS). Table 1 presents the number of species and elementary reactions included in the two mechanisms used in the present study (*ACR55* and *Updated HP-Mech*). Simulations have been performed using the ANSYS CHEMKIN-PRO software [17]. For the problem of ignition of homogeneous mixture, identification of the ignition delay time in simulations is commonly based on either the maximum of the hydroxyl radical (OH) concentration or the temperature inflection point criterion. A careful processing of our results has shown that the second criterion is more appropriate for the present problem and conditions; thus, all computed ignition delay times reported subsequently correspond to a zero second derivative of the temperature in time. Representative computational results for ignition delay times are presented in Figure 1 (φ = 0.5 and 1.0 for pressure of 50 atm).

Table 1. Number of species and elementary reactions included in the two mechanisms used in the present study.

Mechanism	Number of species	Number of reactions
ACR 55	18	55 (**irreversible**)
Updated Hp-Mech	131	899 (**reversible**)

(a)

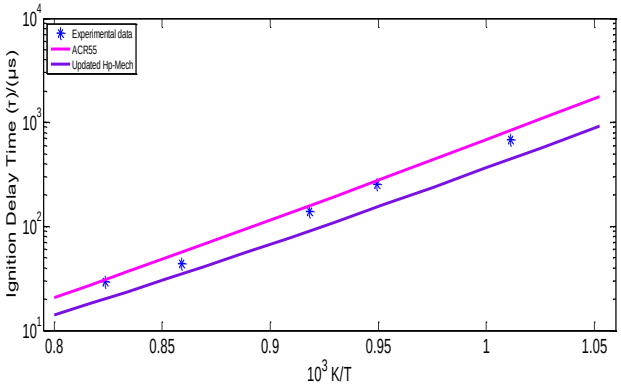

(b)

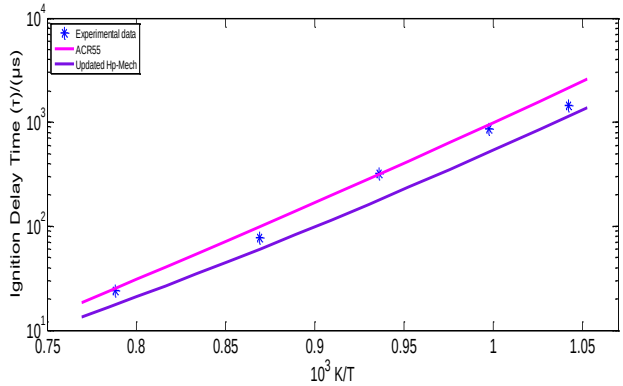

Figure 1. Ignition delay time profiles versus initial temperature for: (a) φ=0.5 and P=50 atm, with mixture composition per volume of 6.544% CH_3OH, 19.634% O_2, and 73.822% N_2. Experimental data from [16]. (b) φ=1.0 and P=50 atm, with mixture composition per volume: 12.28% CH_3OH, 18.43 % O_2, and 69.29 % N_2. Experimental data from [16].

Representative computed speciation profiles are shown in Figure 2 (P=20 atm and φ=0.5) and Figure 3 (P=100 atm, for φ=1.0). Finally, computed laminar flame speeds of methanol−air mixtures at P=5 bar and unburned mixture temperature T_{un}=373 K are shown in Figure 4.

(a)

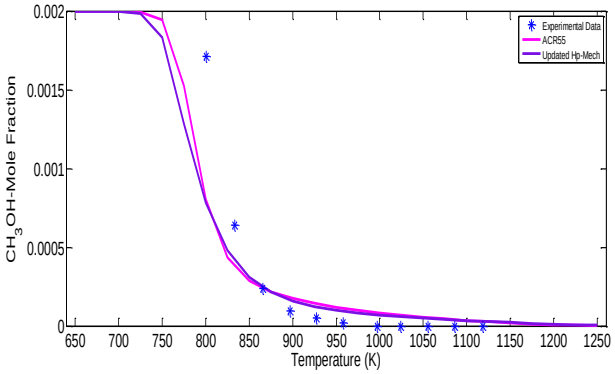

(b)

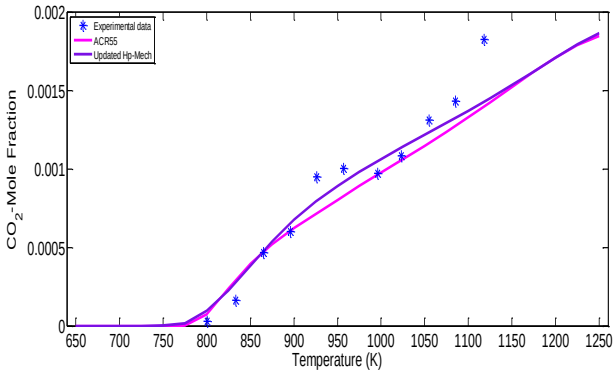

Figure 2. Mole fraction temperature profiles of: (a) CH_3OH. (b) CO_2. Here, combustion at PSR condtions is considered, at P=20 atm and φ=0.5. Mixture composition per volume: 0.2% CH_3OH, 0.6% O_2, and 99.2% N_2. Experimental data from [16].

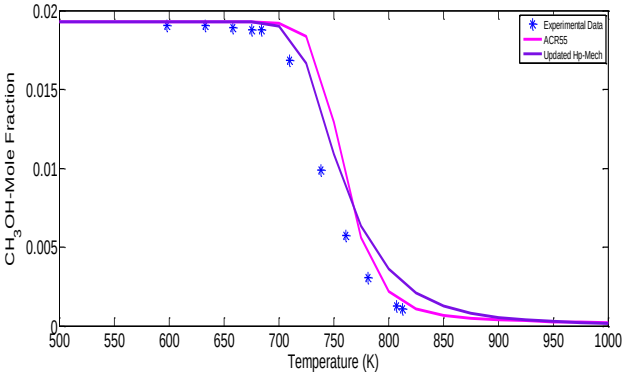

Figure 3. Mole fraction temperature profiles of CH_3OH. Here, combustion at PSR condtions is considered, at P=100 atm and φ=1. Mixture composition per volume: 1.93% CH_3OH, 2.9% O_2, and 95.17 %. Experimental data from [13].

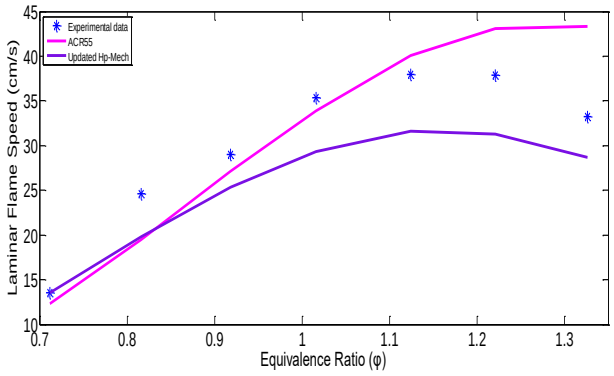

Figure 4. Laminar flame speed versus equivalence ratio, for CH_3OH−air mixtures at P=5 bar and T_{un}=373 K. Experimental data from [14].

Careful inspection of the results presented in Figures 1-4 indicates that the *ACR55* mechanism accurately predicts ignition delay times for all operational conditions and stoichiometries considered. Additionally, the results of the *ACR55* mechanism are in very good agreement with the experimental data for the JSR experiments, and are also consistent with the corresponding computational results of the *Updated HP-Mech* mechanism. Finally, for the pressure of P=5 bar considered (Figure 4), the *ACR55* mechanism accurately reproduces laminar flame speeds for lean mixtures (φ=0.7-1.0), and starts deviating for experimental results for rich mixtures (φ=1.0-1.4).

To quantify the deviation of computational results of the *ACR55* from the experimental data, an average relative error has been calculated for each dataset. Table 2 presents the values of the computed average relative error for the *ACR55* mechanism, as well as for the *Updated HP-Mech* mechanism. These values verify the validity of the *ACR55* mechanism for methanol combustion. It is noted that, in a number of cases, the *ACR55* mechanism outperforms the *Updated HP-Mech* mechanism, which is remarkable considering that the *ACR55* mechanism includes only 18 species and 55 irreversible reactions. In conclusion, for all three reference problems, the *ACR55* mechanism consistently reproduces the experimental data across the entire range of parameters considered. Thus, the *ACR55* mechanism is adopted for further investigation of CH_3OH combustion in an s-CO_2 environment.

Table 2. Average Relative Error of the *Updated HP-Mech* and *ACR55* mechanisms for the three prototype problems of the present study: (i) Ignition of homogeneous mixture, (ii) Combustion in PSR conditions, and (iii) Premixed laminar flame.

#	Data Set	Average Relative Error (%)	Average Relative Error (%)
		Updated HP-Mech.	*ACR55*
Experimental data from [16]			
1	IDT, P=50 atm, φ=0.5	10.2	2.1
2	IDT, P=50 atm, φ=1.0	2.9	6.4
3	PSR, P=20 atm, φ=0.5, CH_3OH	28.6	32.3
4	PSR, P=20 atm, φ=0.5, CO_2	8.5	11.3
Experimental data from [13]			
5	PSR, P=100 atm, φ=1.0, CH_3OH	27.7	21
Experimental data from [14]			
6	LFS, P=5.0 bar, T_{un} = 373 K	9	33.2

SUPERCRITICAL COMBUSTION: PSR AND LAMINAR FLAME

Very high pressure combustion is an emerging technique for enhancing thermodynamic efficiency and reducing pollutant emissions. To this end, a new innovative concept regarding combustion in engineering applications, such as gas turbines and marine engines, consist in the adaptation of the supercritical fluids (SCFs). Supercritical fluids exhibit properties that differ significantly from those at subcritical states. The critical point of CO_2 corresponds to a pressure of 73.8 bar and a temperature of 304 K (31.1 °C) (Budisa and Schulze-Makuch (2014) [18]). Supercritical carbon dioxide (s-CO_2) is a nonpolar medium with a high quadrupole moment. Close to the critical pressure, slight changes in thermal parameters can significantly impact the local density.

In this context, and considering the existing implementation of methanol use under s-CO_2 conditions for gas turbines, calculations were conducted for methanol combustion at PSR conditions and premixed laminar flame for two cases: (a) conventional combustion with N_2 as diluent, and (b) the innovative concept with s-CO_2

as diluent, under identical conditions of temperature, pressure and stoichiometry; these conditions are representative of gas turbine and marine dual-fuel engine operation. In particular, the following range of conditions has been considered: pressures of 175–250 atm, initial temperatures of 1300–1800 K, and values of equivalence ratio from 0.4 to 2.0. In this Section, the *ACR55* mechanism is utilized to quantify the effect of s-CO_2 conditions on the combustion of CH_3OH–O_2 mixtures. It is noted that, based on a thorough literature review, no experimental data pertinent to methanol combustion at the above (supercritical s-CO_2) conditions are available. Thus, considering also the mechanism assessment study reported in the previous Section, the present results with the reduced *ACR55* mechanism are referenced to those of the *Updated HP-Mech* detailed mechanism.

For PSR combustion, representative computational results (profiles of CH_3OH and CO_2 versus temperature) are shown in Figure 5 (P=175 bar and φ=0.5) and Figure 6 (P=220 bar and φ=1.5), considering the presence of either N_2 or s-CO_2.

(a)

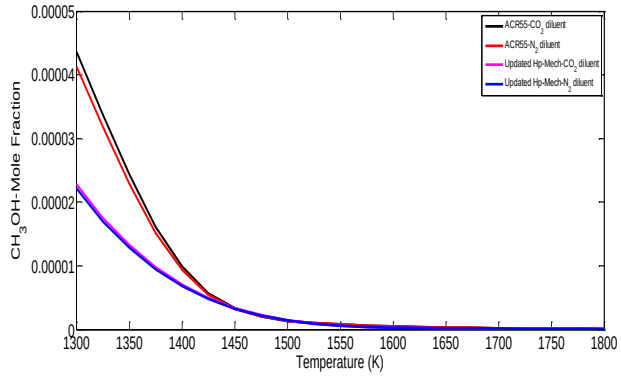

(b)

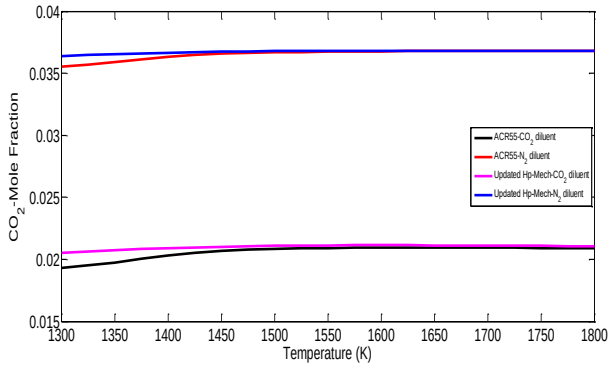

Figure 5. Mole fraction temperature profiles of: (a) CH_3OH. (b) CO_2. Here, combustion at PSR condtions is considered, at P=175 bar and φ=0.5. Mixture composition per volume: 3.75% CH_3OH, 11.25% O_2, 85% CO_2/N_2.

(a)

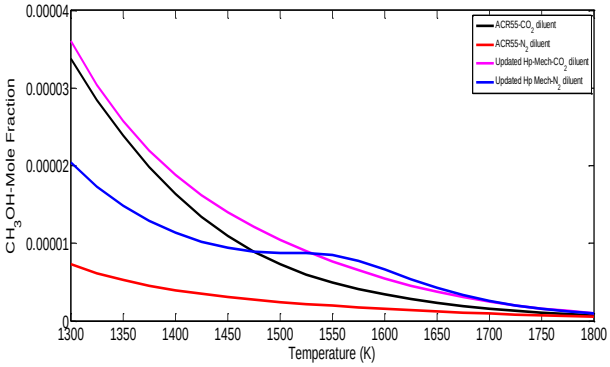

(b)

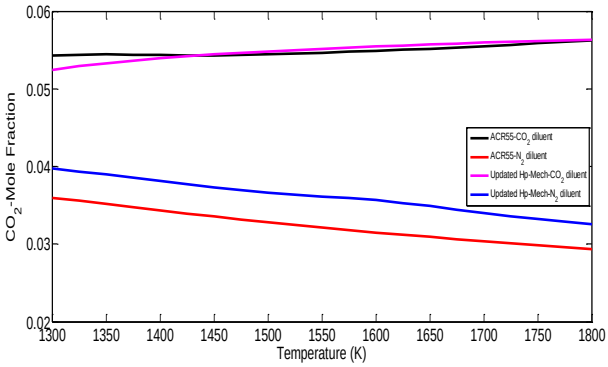

Figure 6. Mole fraction temperature profiles of: (a) CH_3OH. (b) CO_2. Here, combustion at PSR condtions is considered, at P=220 bar and φ=1.5. Mixture composition per volume: 7.5% CH_3OH, 7.5% O_2, 85% CO_2/N_2.

A detailed examination of the results presented in Figures 5 and 6 demonstrates three main features regarding combustion under PSR conditions. First, the fuel is fully consumed across the entire temperature range considered, for all cases studied, both in N_2 and s-CO_2 supercritical conditions. It is underlined that, for the case of s-CO_2, the CO_2 mole fraction presented in Figures 5(b) and 6(b) refers to either the production or consumption of CO_2 in the process, with reference to the initial concentration of 85% CO_2 at the inlet. In particular, for lean mixtures (Figure 5(b)), the CO_2 produced under s-CO_2 conditions is significantly less than the produced in the presence of N_2. For rich mixtures (Figure 6(b)) the presented CO_2 for the s-CO_2 case corresponds to values of *consumption* of CO_2 with reference to the initial 85% CO_2 concentration. The results of Figure 6(b) verify that, for rich mixtures, the s-CO_2 environment also results in enhanced reduction of CO_2, in comparison to the conventional N_2 environment.

Finally, computed laminar flame speeds of methanol−air mixtures are presented in Figure 7, for the following conditions of unburned mixture: (a) P=220 atm, T_{un}=700 K, and (b) P=200 atm, T_{un}=1800 K.

(a)

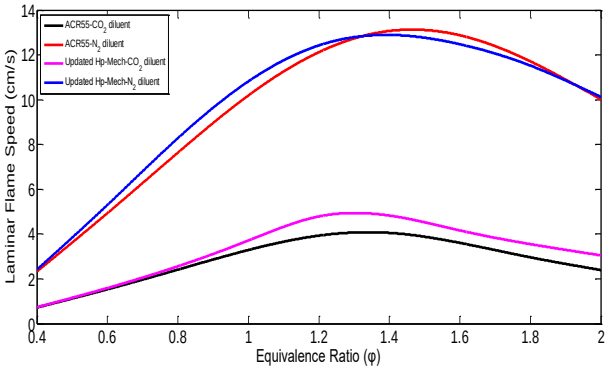

(b)

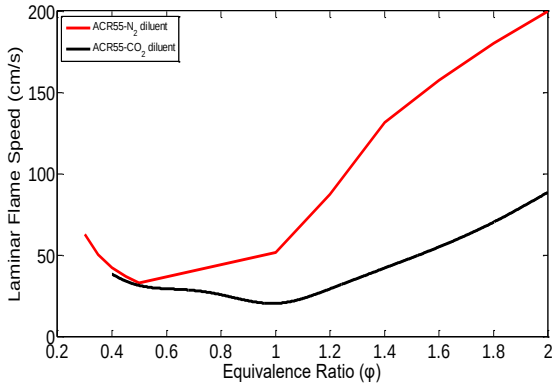

Figure 7. Laminar flame speed versus equivalence ratio for CH_3OH combustion in N_2/CO_2, at (a) P = 220 atm and T_{un} = 700 K, (b) P = 200 atm and T_{un} = 1800 K.

The results shown in Figure 7(a) confirm that there is no substantial deviation in the predictions of laminar flame speed with the *ACR55* and *Updated HP-Mech* mechanisms, for both N_2 and CO_2 dilution. Overall, laminar flame speeds in an N_2 environment are higher than those in the s-CO_2 environment. In particular, for the case of unburned mixture temperature T_{un}=700 K, laminar flame speed is significantly higher (by up to about 200%) for all pressures (P=175-250 atm) and equivalence ratios considered (φ=0.4-2.0). On the other hand, for unburned mixture temperature T_{un}=1800 K, laminar flame speed values are comparable for N_2 and s-CO_2 dilution regarding lean mixtures (Figure 7(b)). The deviation increases as the mixture becomes increasingly richer, characterized by higher values of N_2 dilution (Figure 7(b)).

CHEMICAL ANALYSIS

The effect of N_2 and CO_2 on PSR concentration profiles and on laminar flame speed, characterized in the previous Section, is analyzed here through Rate of Production (ROP) analysis.

As shown in the previous Section, the production of CO_2 in PSR is higher for CH_3OH-N_2 mixtures; the effect is analyzed here via ROP analysis for the representative case φ=0.5, P=220 bar, T=1500 K. For premixed laminar flame problem, laminar flame speed has been shown to be higher for N_2-dilution, in comparison to s-CO_2-dilution; the effect is analyzed for the representative case φ=0.5, P=220 atm and T_{un}=700 K.

Tables 3 and 4 present the absolute and normalized consumption rates, respectively, of the dominant in terms of fuel consumption elementary reactions, both for N_2-dilution and s-CO_2-dilution. The data demonstrate that the most important reactions for CH_3OH consumption are R49 and R50, with their relative contribution remaining the same for the two diluents considered (Table 4). Thus, the main radicals controlling CH_3OH consumption are the oxygen radical (O) and the hydroxyl radical (OH). Further, Tables 5 and 6 present the absolute and normalized production rates, respectively, of the dominant in terms of OH production elementary reactions, both for N_2-dilution and s-CO_2-dilution. The two Tables illustrate that, for s-CO_2 dilution, the most important reactions for OH production are R9, R13, R33, R39 and R49; for N2 dilution, the above elementary reactions, except R33, dominate OH production.

Table 3. Absolute consumption rates for the dominant CH_3OH consumption elementary reactions (P=220 bar, T=1500 K and φ=0.5).

Reactions	**Absolute rate (moles/cc-s)**	
CH_3OH consumption	**CO_2 diluent**	**N_2 diluent**
$CH_3OH(+M)=>CH_3+OH(+M)$ (R44)	$1.96\cdot10^{-6}$	$1.94\cdot10^{-6}$
$CH_3OH+O=>CH_3O+OH$ (R48)	$6.65\cdot10^{-6}$	$6.67\cdot10^{-6}$
$CH_3OH+O=>CH_2OH+OH$ (R49)	$1.00\cdot10^{-4}$	$1.01\cdot10^{-4}$
$CH_3OH+OH=>CH_2OH+H_2O$ (R50)	$4.32\cdot10^{-5}$	$4.30\cdot10^{-5}$

Table 4. Normalized consumption rates for the dominant CH_3OH consuming elementary reactions (P=220 bar, T=1500 K and φ=0.5).

Reactions	**Normalized rate**	
CH_3OH consumption	**CO_2 diluent**	**N_2 diluent**
$CH_3OH(+M)=>CH_3+OH(+M)$ (R44)	0.013	0.013
$CH_3OH+O=>CH_3O+OH$ (R48)	0.043	0.044
$CH_3OH+O=>CH_2OH+OH$ (R49)	0.656	0.658
$CH_3OH+OH=>CH_2OH+H_2O$ (R50)	0.282	0.281

Table 5. Absolute production rates for the dominant OH producing elementary reactions (P=220 bar, T=1500 K and φ=0.5).

Reactions		Absolute rate (moles/cc-s)	
OH production		**CO_2 diluent**	**N_2 diluent**
$H+H_2O=>H_2+OH$	(R4)	$7.80\cdot10^{-5}$	$7.88\cdot10^{-5}$
$H_2+O=>H+OH$	(R5)	$1.59\cdot10^{-5}$	$1.61\cdot10^{-5}$
$O_2+H=>O+OH$	(R9)	$2.56\cdot10^{-4}$	$2.58\cdot10^{-4}$
$H_2O_2(+M)=>2OH(+M)$	(R13)	$1.48\cdot10^{-4}$	$1.47\cdot10^{-4}$
$CH_2O+O=>HCO+OH$	(R18)	$5.32\cdot10^{-5}$	$5.35\cdot10^{-5}$
$CO_2+H=>CO+OH$	(R33)	$1.49\cdot10^{-4}$	-
$H_2O+O_2=>OH+HO_2$	(R39)	$1.31\cdot10^{-4}$	$1.31\cdot10^{-4}$
$CH_3OH+O=>CH_2OH+OH$	(R49)	$1.00\cdot10^{-4}$	$1.01\cdot10^{-4}$

Table 6. Normalized production rates for the dominant OH producing elementary reactions (P=220 bar, T=1500 K and φ=0.5).

Reactions		Normalized rate	
OH production		**CO_2 diluent**	**N_2 diluent**
$H+H_2O=>H_2+OH$	(R4)	0.083	0.098
$H_2+O=>H+OH$	(R5)	0.017	0.02
$O_2+H=>O+OH$	(R9)	0.271	0.322
$H_2O_2(+M)=>2OH(+M)$	(R13)	0.157	0.183
$CH_2O+O=>HCO+OH$	(R18)	0.057	0.067
$CO_2+H=>CO+OH$	(R33)	0.158	-
$H_2O+O_2=>OH+HO_2$	(R39)	0.139	0.163
$CH_3OH+O=>CH_2OH+OH$	(R49)	0.107	0.126

Analysis of the present results indicates that, for s-CO_2 dilution, the absolute total production rate of CO_2 is $3.01\cdot10^{-4}$ moles/cc-s, and $1.59\cdot10^{-4}$ moles/cc-s for the N_2 dilution.

$CO+OH=>CO_2+H$ (R32)

Regarding CO_2 consumption, it is noted that, for s-CO_2 dilution, consumption is dominated by the contribution of elementary reaction R33, yielding a high total consumption rate of $1.49\cdot10^{-4}$ moles/cc-s. For N_2 dilution, the total consumption rate is smaller by nearly two orders of magnitude, equal to $6.33\cdot10^{-6}$ moles/cc-s; this results in a CO_2 concentration higher than that of s-CO_2 dilution by nearly a factor of two.

$CO_2+H=>CO+OH$ (R33)

Next, the analysis of the laminar flame case (φ=0.5, P=220 atm, T_{un}=700 K) is presented. Figure 8 presents the absolute consumption rates of the dominant CH_3OH consumption elementary reactions at conditions of φ=0.5, P=220 atm, T_{un}=700 K, close to the center of the computational domain considered (x=0.1 cm). Figure 8 demonstrates that the dominant radical for CH_3OH consumption is OH, via elementary reaction R50:

$CH_3OH + OH = CH_2OH + H_2O$ (R50)

The total absolute rate of CH_3OH consumption is an order of magnitude smaller in the case of the CH_3OH-s-CO_2 mixture in comparison to the CH_3OH-N_2 mixture (Figure 8).

(a)

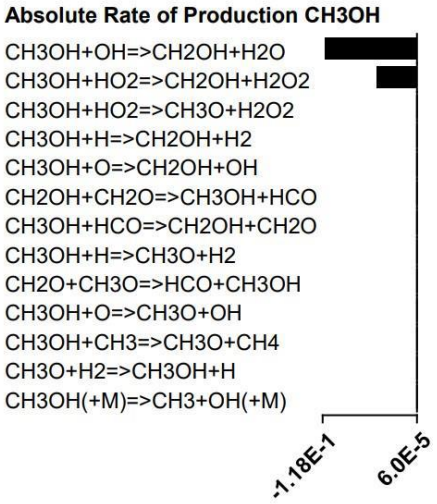

(b)

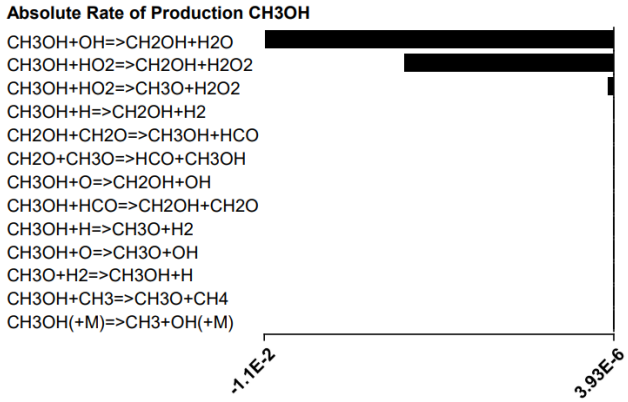

Figure 8. Absolute consumption rates for the dominant CH_3OH elementary reactions, for (a) CH_3OH-N_2 mixture, (b) CH_3OH-s-CO_2 mixture (φ=0.5, P=220 atm, and T_{un}=700 K), at axial position x=0.1 cm.

Figure 9 presents the absolute production rates of the dominant OH producing elementary reactions for the two cases investigated (N_2, s-CO_2 dilution). In both cases, the most important reaction contributing to the production of OH is the following:

H_2O_2 (+M) => 2OH (+M) (R13)

The absolute rate of OH production in R13 is $2.18\cdot10^{-1}$ moles/cc-s for the case of the CH_3OH-N_2 mixture, while it is $1.98\cdot10^{-2}$ moles/cc-s for the CH_3OH-s-CO_2 mixture (an order of magnitude lower).

The higher rate of OH production for the CH_3OH-N_2 mixture is related to the higher production rate of H_2O_2, which is produced mainly through the following elementary reactions:

$CH_3OH + HO_2 \Rightarrow CH_2OH + H_2O_2$ (R52)

$2HO_2 \Rightarrow H_2O_2 + O_2$ (R26)

$CH_2O + HO_2 \Rightarrow HCO + H_2O_2$ (R22)

The total absolute rate of H_2O_2 production is $1.17 \cdot 10^{-1}$ moles/cc-s for the CH_3OH-N_2 mixture, and is an order of magnitude higher than the respective rate for the CH_3OH-s-CO_2 mixture ($1.53 \cdot 10^{-2}$ moles/cc-s).

The higher rate of H_2O_2 production in the CH_3OH-N_2 mixture should be associated with the higher production rate of HO_2, which is produced mainly through the following elementary reactions:

$CH_2OH + O_2 \Rightarrow CH_2O + HO_2$ (R1)

$HCO + O_2 \Rightarrow CO + HO_2$ (R34)

The total absolute rate of HO_2 production is $2.79 \cdot 10^{-1}$ moles/cc-s for the CH_3OH-N_2 mixture, and is an order of magnitude higher than the corresponding rate of the CH_3OH-s-CO_2 mixture, which is $2.84 \cdot 10^{-2}$ moles/cc-s.

The pathway analyzed above leads to a higher laminar flame speed in the case of the CH_3OH-N_2 mixture (see Figure 7(a)).

(a)

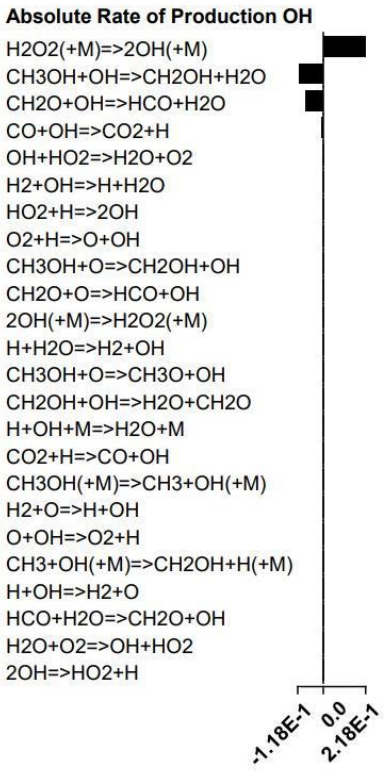

(b)

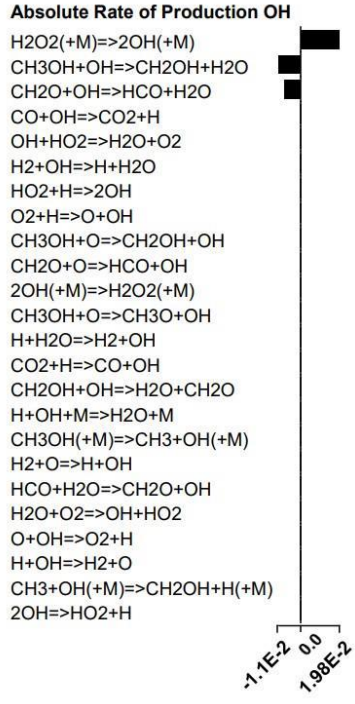

Figure 9. Absolute production rates for the OH-producing elementary reactions for (a) CH_3OH-N_2 mixture, (b) CH_3OH-s-CO_2 mixture (φ=0.5, P=220 atm, and T_{un}=700 K), at axial position x=0.1cm.

CONCLUSIONS

The aim of the present study has been the comprehensive computational investigation of CH_3OH combustion under CO_2 supercritical conditions (s-CO_2). To this end, an approach consisting of the following steps has been undertaken: (**a**) assessment of a reduced order chemical kinetic mechanism, namely, *ACR55* of Pichler & Nilsson (2018), consisting of 18 species and 55 irreversible reactions, against experimental data of: (i) laminar flame speeds, (ii) ignition delay times, and (iii) speciation data from JSRs, for a wide range of conditions, including high pressures. The results of the *ACR55* mechanism have been also evaluated against the computational results of the *Updated HP-Mech* of Wang et al. detailed mechanism (2022), consisting of 131 species and 899 reversible reactions. Also, the accuracy of computational results has been characterized by comparing the relative error of the *ACR55* mechanism results with experiments and the corresponding relative difference with the *Updated HP-Mech*. (**b**) Investigation of the effect of CO_2 as diluent for combustion at PSR conditions and premixed laminar flame by considering: (i) conventional combustion with N_2 as diluent, and (ii) combustion with s-CO_2 as diluent, at conditions representative of gas turbine and marine dual-fuel engine operation. (**c**) Identification of dominant pathways by means of ROP analysis.

The main findings of the present work can be summarized as follows:

i. Combustion at PSR conditions: The two mechanisms produce comparable results in the entire range of conditions investigated. The fuel is fully consumed for all cases studied. With respect to the initial concentration of 85% CO_2, for lean and stoichiometric mixtures, the concentration of the produced CO_2 in the case of s-CO_2 as diluent is lower in comparison to that of N_2 dilution. For rich mixtures, also with respect to the initial concentration of 85% CO_2, the combustion at s-CO_2 environment results in values of *consumption* of CO_2 which verify the reduction of CO_2 emissions in comparison to the ones of N_2 dilution.

ii. Premixed laminar flames: For a wide variation of pressure (P=175-250 atm), for T_{un}=600 K, 700 K, the laminar flame speed is significantly higher (about 200%) for N_2 dilution, for all stoichiometries considered (φ=0.4-2.0). For T_{un}=1800 K and lean mixtures, the laminar flame speed is higher for N_2 dilution, however the differences are milder; for rich mixtures, the laminar flame speed is substantially higher for N_2 dilution.

The important effects of CH_3OH combustion at s-CO_2 conditions have been interpreted by means of ROP analysis.

The present work constitutes an initial approach to understanding, from a fundamental basis, the complex phenomenon of combustion at CO_2 supercritical conditions. The outcome of the present investigation can be used as a backbone for a deeper understanding of combustion at extreme conditions.

ACKNOWLEDGMENTS

All authors acknowledge the financial support of the Highly Efficient Super Critical ZERO eMission Energy System (HERMES) project (HORIZON-CL5-2021-D3-03-02 - 632487).

REFERENCES

[1] MEPC (Marine Environment Protection Committee). 2023. 2023 IMO Strategy on Reduction of GHG Emissions from Ships. MEPC.377(80). London: International Maritime Organization.

[2] MEPC (Marine Environment Protection Committee). 2008. Amendments to the annex of the protocol of 1997 to amend the international convention for the prevention of pollution from ships, 1973, as modified by the protocol of 1978 relating thereto (revised MARPOL annex VI). MEPC.176(58). London: International Maritime Organization.

[3] MEPC (Marine Environment Protection Committee). 2019. 2019 Guidelines for consistent implementation of the 0.50% sulphur limit under MARPOL annex VI. MEPC.320(74). London: International Maritime Organization.

[4] Topic, T., Murphy, A.J., Pazouki, K. and Norman, R. (2023). “NOx Emissions Control Area (NECA) scenario for ports in the North Adriatic Sea”, Journal of Environmental Management 344 (Oct): 118712. https://doi.org/10.1016/j.trd.2023.103957

[5] White, T.M., Bianchi, G., Ghai, L, Tassou, S.A. and Sayma, A.I. (2021). “Review of supercritical CO_2 technologies and systems for power generation”. Applied Thermal Engineering, 185: 116447. https://doi.org/10.1016/j.applthermaleng.2020.116447.

[6] Hacks, A., Sebastian, S., Dohmen, H.J., Benra, F.-K. and Brillert, D., (2018). “Turbomachine

Design for Supercritical Carbon Dioxide Within the sCO_2-HeRo.eu Project", Journal of Engineering for Gas Turbines and Power 140 (12): 121017. https://doi.org/10.1115/1.4040861.

[7] Sharma, I., Shah, V. and Shah, M. (2022). "A comprehensive study on production of methanol from wind energy", Environmental Technology & Innovation 28: 102589. https://doi.org/10.1016/j.eti.2022.102589.

[8] Bellan, J. (2000). "Supercritical (and subcritical) fluid behavior and modeling: drops, streams, shear and mixing layers, jets and sprays", Progress in Energy and Combustion Science (26):329-366. https://doi.org/10.1016/S0360-1285(00)00008-3.

[9] Yang, V. (2000). "Modeling of supercritical vaporization, mixing, and combustion processes in liquid-fueled propulsion systems", Proceedings of the Combustion Institute 28(1):925-942. https://doi.org/10.1016/S0082-0784(00)80299-4.

[10] Karvounis, P., Theotokatos, G., Patil, C., Xiang, L. and Ding, Y. (2025). "Parametric investigation of diesel–methanol dual fuel marine engines with port and direct injection", Fuel 38 (Part B): 133441. https://doi.org/10.1016/j.fuel.2024.133441.

[11] MEPC (Marine Environment Protection Committee). 2023. Reduction of GHG emissions from ships: Report on the study on the readiness and availability of low- and zero-carbon ship technology and marine fuels. MEPC.80/INF.10. London: International Maritime Organization.

[12] Pichler, C. and Nilsson, E.J.K. (2018). "Reduced Kinetic Mechanism for Methanol Combustion in Spark-Ignition Engines", Energy and Fuels (32):12805-12813. https://pubs.acs.org/doi/10.1021/acs.energyfuels.8b02136.

[13] Wang, Z., Zhao, H., Yan, C., Lin, Y., Lele, A. D., Xu, W., Rotavera, B., Jasper, A.W., Klippenstein, S.J. and Ju, Y. (2022). "Methanol oxidation up to 100 atm in a supercritical pressure jet-stirred reactor", Proceedings of the Combustion Institute 39 (1): 445-453. https://doi.org/10.1016/j.proci.2022.07.068.

[14] Zhang, Z., Huang, Z., Wang, X., Xiang, J., Wang, X. and Miao, H. (2008). "Measurements of laminar burning velocities and Markstein lengths for methanol–air–nitrogen mixtures at elevated pressures and temperatures", Combustion and Flame 155 (3): 358–368. https://doi.org/10.1016/j.combustflame.2008.07.005.

[15] Beeckmann, J., Cai, L. and Pitsch, H. (2014). "Experimental investigation of the laminar burning velocities of methanol, ethanol, n-propanol, and n-butanol at high pressure", Fuel 117 (Part A): 340–350. https://doi.org/10.1016/j.fuel.2013.09.025.

[16] Burke, U., Metcalfe, W.K., Burke, S.M., Heufer, K.A., Dagaut, P. and Currana, H.J. (2016). "A detailed chemical kinetic modeling, ignition delay time and jet-stirred reactor study of methanol oxidation", Combustion and Flame 165 (Mar): 125–136. http://dx.doi.org/10.1016/j.combustflame.2015.11.004.

[17] ANSYS CHEMKIN-PRO. (2022). ANSYS Reaction Design: San Diego.

[18] Budisa, N. and Schulze-Makush, D. (2014). "Supercritical Carbon Dioxide and Its Potential as a Life-Sustaining Solvent in a Planetary Environment", Life 4(3):331-340. https://doi.org/10.3390/life4030331.